



Investigation of Interfacial Phenomena During Condensation of Humid Air on a Horizontal Substrate

Akhilesh Tiwari, Jean-Pierre Fontaine, Alain Kondjoyan, Jean-Bernard Gros,
Christophe Vial, Claude-Gilles Dussap

► To cite this version:

Akhilesh Tiwari, Jean-Pierre Fontaine, Alain Kondjoyan, Jean-Bernard Gros, Christophe Vial, et al.. Investigation of Interfacial Phenomena During Condensation of Humid Air on a Horizontal Substrate. Oil & Gas Science and Technology - Revue d'IFP Energies nouvelles, 2014, 69 (3), pp.445-456. 10.2516/ogst/2013138 . hal-01933386

HAL Id: hal-01933386

<https://hal.science/hal-01933386>

Submitted on 23 Nov 2018

HAL is a multi-disciplinary open access archive for the deposit and dissemination of scientific research documents, whether they are published or not. The documents may come from teaching and research institutions in France or abroad, or from public or private research centers.

L'archive ouverte pluridisciplinaire **HAL**, est destinée au dépôt et à la diffusion de documents scientifiques de niveau recherche, publiés ou non, émanant des établissements d'enseignement et de recherche français ou étrangers, des laboratoires publics ou privés.



Distributed under a Creative Commons Attribution 4.0 International License



This paper is a part of the hereunder thematic dossier published in OGST Journal, Vol. 69, No. 3, pp. 379-499 and available online [here](#)

Cet article fait partie du dossier thématique ci-dessous publié dans la revue OGST, Vol. 69, n°3 pp. 379-499 et téléchargeable [ici](#)

DOSSIER Edited by/Sous la direction de : **J.-F. Argillier**

IFP Energies nouvelles International Conference / Les Rencontres Scientifiques d'IFP Energies nouvelles Colloids 2012 – Colloids and Complex Fluids: Challenges and Opportunities Colloids 2012 – Colloïdes et fluides complexes : défis et opportunités

Oil & Gas Science and Technology – Rev. IFP Energies nouvelles, Vol. 69 (2014), No. 3, pp. 379-499

Copyright © 2014, IFP Energies nouvelles

- | | |
|--|---|
| <p>379 >Editorial
H. Van Damme, M. Moan and J.-F. Argillier</p> <p>387 >Formation of Soft Nanoparticles via Polyelectrolyte Complexation: A Viscometric Study
Formation de nanoparticules molles par complexation de polyélectrolytes : une étude viscosimétrique
C. Rondon, J.-F. Argillier, M. Moan and F. Leal Calderon</p> <p>397 >How to Reduce the Crack Density in Drying Colloidal Material? Comment réduire la densité de fractures dans des gels colloïdaux ?
F. Boulogne, F. Giorgiutti-Dauphiné and L. Pauchard</p> <p>405 >Adsorption and Removal of Organic Dye at Quartz Sand-Water Interface Adsorption et désorption d'un colorant organique à l'interface sable de quartz-eau
A. Jada and R. Ait Akbour</p> <p>415 >Freezing Within Emulsions: Theoretical Aspects and Engineering Applications
Congélation dans les émulsions : aspects théoriques et applications techniques
D. Clausse and C. Dalmazzone</p> <p>435 >Effect of Surfactants on the Deformation and Detachment of Oil Droplets in a Model Laminar Flow Cell
Étude de l'effet de tensioactifs sur la déformation et le détachement de gouttes d'huiles modèles à l'aide d'une cellule à flux laminaire
V. Fréville, E. van Hecke, C. Ernenwein, A.-V. Salsac and I. Pezron</p> | <p>445 > Investigation of Interfacial Phenomena During Condensation of Humid Air on a Horizontal Substrate
Investigation de phénomènes interfaciaux au cours de la condensation d'air humide sur un substrat horizontal
A. Tiwari, J.-P. Fontaine, A. Kondjoyan, J.-B. Gros, C. Vial and C.-G. Dussap</p> <p>457 > Microfluidic Study of Foams Flow for Enhanced Oil Recovery (EOR)
Étude en microfluidique de l'écoulement de mousses pour la récupération assistée
N. Quennouz, M. Ryba, J.-F. Argillier, B. Herzhaft, Y. Peysson and N. Pannacci</p> <p>467 > Non-Aqueous and Crude Oil Foams
Mousses non aqueuses et mousses pétrolières
C. Blázquez, É. Emond, S. Schneider, C. Dalmazzone and V. Bergeron</p> <p>481 > Development of a Model Foamy Viscous Fluid
Développement d'un modèle de dispersion gaz-liquide de type mousse liquide visqueuse
C. Vial and I. Narchi</p> <p>499 > Erratum
D.A. Saldana, B. Creton, P. Mouglin, N. Jeuland, B. Rousseau and L. Starck</p> |
|--|---|

Investigation of Interfacial Phenomena During Condensation of Humid Air on a Horizontal Substrate

Akhilesh Tiwari¹, Jean-Pierre Fontaine^{1*}, Alain Kondjoyan², Jean-Bernard Gros¹,
Christophe Vial¹ and Claude-Gilles Dussap¹

¹ Clermont Université, Université Blaise Pascal, Institut Pascal – axe GePEB (UMR 6602), BP10488, 63000 Clermont Ferrand - France

² Institut National de la recherche Agronomie (INRA), UR Qualité des Produits Animaux, 63122 Saint-Genès-Champanelle - France

e-mail: akhilesh.tiwari77@gmail.com - j-pierre.fontaine@univ-bpclermont.fr - alain.kondjoyan@clermont.inra.fr
j-bernard.gros@univ-bpclermont.fr - christophe.vial@univ-bpclermont.fr - c-gilles.dussap@univ-bpclermont.fr

* Corresponding author

Résumé — Investigation de phénomènes interfaciaux au cours de la condensation d'air humide sur un substrat horizontal — La condensation d'air humide sur des substrats solides peut se produire

dans beaucoup d'applications et ce phénomène est reconnu comme un des problèmes les plus difficiles à traiter pour l'amélioration de la qualité de l'air dans un espace clos. L'étude présentée a été motivée par l'étude du couplage entre la ventilation et la condensation à l'intérieur d'écosystèmes clos artificiels (CELSS, Controlled Ecological Life Support Systems), puisque ce couplage joue un rôle important sur la croissance de plantes supérieures dans des serres et sur les conditions de vie dans des cabines spatiales habitées, particulièrement pour les vols de longue durée ou les futures bases spatiales. Il est bien connu que l'augmentation des échanges gazeux au niveau des feuilles et la croissance des plantes dépendent des conditions organoleptiques et/ou des facteurs thermo-physiques environnants. Une convection insuffisante autour des plantes et de la condensation sur les feuilles limitent la croissance en supprimant la diffusion de gaz dans la couche limite de la feuille diminuant ainsi les taux de photosynthèse et de transpiration. Ainsi, l'optimisation d'un CELSS nécessitera le contrôle du flux d'air et du transfert gaz/liquide concomitant aux interfaces des plantes. Les modèles expérimentaux et théoriques de CELSS exigent une compréhension complète des transferts gaz/liquide de l'échelle microscopique à l'échelle macroscopique. Un dispositif expérimental a été développé en gravité terrestre pour évaluer les coefficients de transfert de matière pour la condensation d'air humide sur des géométries spécifiques dans des conditions environnementales contrôlées précisément. Le but était d'établir des corrélations entre les flux de matière et de chaleur, l'humidité relative et l'écoulement moyen pour le développement de modèles théoriques basés sur des coefficients de transfert locaux. Les expériences ont été exécutées à température ambiante, avec une humidité relative comprise entre 35 et 70 % et pour une gamme de vitesse de 1,0 à 3,0 m.s⁻¹.

Abstract — Investigation of Interfacial Phenomena During Condensation of Humid Air on a Horizontal Substrate — The condensation phenomenon of humid air on solid substrates can occur in many applications, and it is known as one of the most difficult problem to deal with for the improvement of the quality of air in a closed environment. The present study was motivated by the investigation of the coupling between ventilation and condensation inside Controlled Ecological

Life Support Systems (CELSS), as it has an important role for higher plants growth in greenhouses and living conditions in manned spacecraft cabins, particularly in long duration space flights or in future space bases. It is well known that the enhancement of the gas exchange with leaves and the growth of plants are dependent on the organoleptic and/or the surrounding thermo-physical factors. Insufficient air movement around plants and condensation on plant leaves generally limit their growth by suppressing the gas diffusion in the leaf boundary-layer thereby decreasing photosynthetic and transpiration rates. Thus, the optimization of a CELSS will require the control of the airflow and concomitant gas/liquid transfer at the plant surfaces. The experimental and theoretical modeling of CELSS requires a comprehensive understanding of the micro to the macro levels of liquid gas phase transfer. Hence, an experimental set-up was developed at 1-g to evaluate the mass transfer coefficients due to condensation of humid air on specific geometries in well controlled environmental conditions. The goal was to establish correlations between the fluxes of mass and heat, the relative humidity and the mean flow for the development of theoretical models based on local transfer coefficients. The experiments were performed at ambient temperature, with a relative humidity between 35-70% and for a velocity range of 1.0-3.0 m.s⁻¹.

NOMENCLATURE

L	Total length (m)
D	Diffusion coefficient (m ² /s)
N	Mean heat flux for surface
T	Temperature (K)
U	Characteristic velocity (m/s)
ρ	Density (kg/m ³)
μ	Dynamic viscosity (Pa.s)
Δ	Difference
Re	Reynolds number
Sc	Schmidt number
a	Ambient
c	controller
d	Dew point
f	Film
l	Liquid
s	Surface
SAT	Saturation
∞	Free stream

INTRODUCTION

The condensation phenomenon of humid air on solid substrates can occur in many applications, and it is known as one of the most difficult problem to deal with for the improvement of the quality of air in a closed environment (space habitat, submarine, operation room, greenhouse, etc.), the habitability of crew compartments or the maintainability of electronic devices. It can cause corrosion, the development of mould and pathogen germs, etc. On glass it affects sun radiation.

The development of Earth like environment inside a closed-system for the progress of Controlled Ecological Life Support Systems (CELSS) is a challenge today. This is a requirement for long-duration exploratory manned missions to fulfil the needs of a crew including nutritional demand, atmosphere regeneration, and psychological support [1, 2]. One of the key elements for CELSS are plants [3-5], as they regenerate ambient air by photosynthesis, help water recovery by transpiration, supply fresh food or nutritional needs for crews and can be used for the recycling of wastes. A maximum of biological materials could be reused for plant cultivation thanks to various effective waste processing techniques [6-8].

The importance of recycling within the spacecraft, with crews consuming the products of autotrophic synthesis, requires exchanges between photoautotrophic organisms, which synthesize organic substances using solar or artificial light, and heterotrophic organisms. Hence, growing plants in space missions is a vital component and its performance in CELSS will be principally dependent on the progress of plant cultivation technology for space and the achievement of associated equipment. The growth of higher plants in a greenhouse is optimized by the environmental conditions among which the influence of ventilation, condensation and evaporation phenomena on solid surfaces: leaves, plants, windows and walls. Moreover, condensation on walls or plant leaves has to be controlled as well as the ambient air for optimized living conditions within the spacecraft, even if the humidity level is not as high as in a greenhouse in order to prevent mould, rot or rust. Furthermore, forced convection is known to be a good solution to prevent condensation while maintaining optimized conditions for life. Hence, the optimization of CELSS requires a global coupled hydrodynamic, heat

and mass transfer modeling that could simulate precisely the atmosphere in spatial greenhouses, or in manned capsules. Further, the coupling with microbiological development models [9] will help for the protection of the crew from nosocomial infections, the optimization of the microclimate prevailing in a space greenhouse and a better control of higher plant growth.

In CELSS, the plant culture will play an important role in food production, CO_2/O_2 conversion, and water purification. Life support for crews in space is dependent on both the amount of food and atmospheric O_2 produced by plants in a limited space. In a closed chamber the enhancement of the gas exchange with leaves and growth of plants would be dependent on several factors, including control of air current. Insufficient air movement around plants generally limits their growth by reducing the gas diffusion in the leaf boundary-layer thereby decreasing photosynthetic and transpiration rates [10, 11]. Airflow affects plant growth through energy and mass transfer, latent heat exchanged through the processes of water evaporation (transpiration) and condensation onto plant surfaces is also directly affected by air movement

Thus, the air flowing over the surface of living objects, plants or humans affects their growth and/or behaviour. Most of their activities require a thorough understanding of the local atmospheric conditions. The agricultural process depends on temperature, light radiation reaching the plant leaves, air velocity, and on the amount of water available in the local atmosphere. The net photosynthetic rate of the plant canopy increases with increasing air velocities inside plant canopies [12].

The present study was motivated by the investigation of the coupling between ventilation (forced convection) and condensation inside CELSS. The experimental and theoretical modeling of CELSS requires a comprehensive understanding of the micro to the macro levels of gas/liquid phase transfer. The purpose of this study was to clarify the basic mechanisms concerning the coupling of heat and mass transfer during phases of condensation or evaporation with a low Reynolds number turbulent flow, as well as the kinetics of the diverse phenomena interacting at different characteristic scales. The goal was to establish correlations between the fluxes of mass and heat, the relative humidity and the mean flow for the development of theoretical models based on local transfer coefficients. These models will later be inserted in numerical simulation software for the prediction of airflow and gas/liquid transfer at solid and/or plant surfaces.

The initial objective of this study was to design a set-up and realize experiments of condensation on a small-size horizontal substrate of controlled temperature

to describe and quantify accurately this heterogeneous transfer which develops. A device regulates the surface temperature below the dew point of the air and thus, leads to condensation phases.

We discuss herein the experimental set-up developed at 1 g to characterize the condensation mass flux on a horizontal flat plate in a controlled wind tunnel environment. We have already performed experiments for the study of velocity profiles and boundary layer thickness on the surface of vertical and horizontal flat plates in dry conditions [13, 14]. This paper presents the results (local mass transfer coefficients) obtained for the condensation of humid air in various conditions when the mean flow velocity varies between 1 and 3 m.s^{-1} . The results show the mass transfer increase with thermal or pressure gradients and, in similar environmental conditions, the raise with the mean flow strength.

1 DEFINITION OF THE EXPERIMENT

1.1 Global Experiment

To generate and control a flux of condensation of wet air on the surface of a flat plate, we have developed a system based on a controlled thermoelectric cooler. The temperature of the plate was kept constant in order to induce a stable flux of condensation on the active plate/air interface and the condensate mass was monitored by continuous precise weighing. The overall device was placed in a vein which hydrodynamics, temperature and humidity fields were controlled [15]. The wind tunnel facility is a closed loop, sealed and highly insulated that generates runoff from nearly laminar to highly turbulent regimes. The characterization of the flow, average speed and fluctuations was performed by hot wire anemometry. Figure 1 gives a photograph of the test chamber and the active condensation unit with water condensate on it.

1.2 Description of Condensation Unit

The condensation unit was prepared after extensive experiments on the flat plate for its size and thickness, choice of metal substrate, choice of heat sink, temperature distribution at the air/solid interface (ceramic surface of the Peltier element or aluminium plate above it) in order to obtain a thermally homogeneous surface (which corresponds to the active side of the plate for condensation) [14, 16].

A square plate (2) of aluminium is bonded to a Peltier module (3) of the same size (5 cm \times 5 cm), as seen in Figure 2b. The other face of the module is bonded to a heat sink (4) for the temperature of this side to be

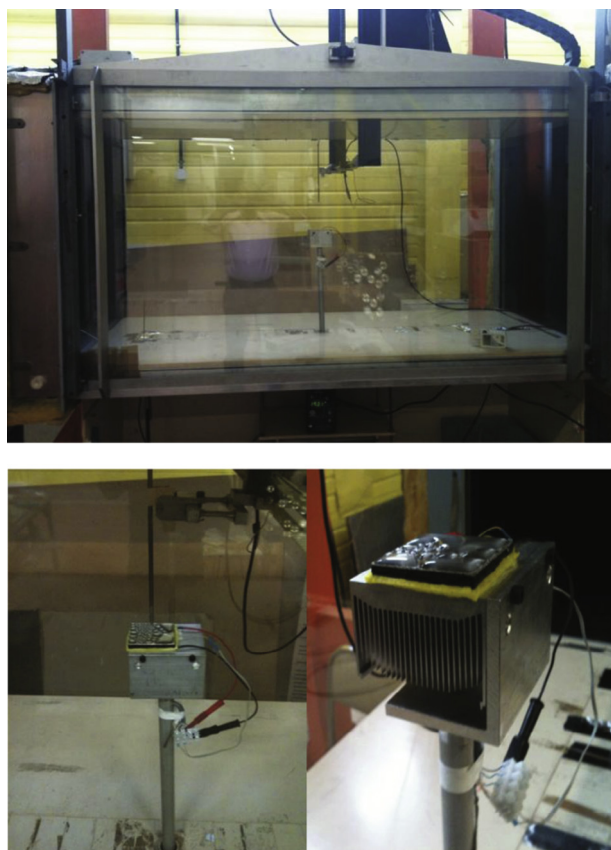


Figure 1

Photograph of test chamber and a close look at the condensing unit in the presence of drops on top of the active surface.

kept close to the ambient temperature (T_a , reference temperature). The temperature of the active surface (T_s) is controlled by a Peltier element which is regulated by means of a thermistor (1) inserted into the small plate and a controller (7) which adjusts the electric current supplied to the Peltier module (Fig. 2a).

The condensation unit is placed horizontally (active horizontal plate) at the centre of the test chamber (upper part of Fig. 2). It is maintained in the measuring chamber by a shaft (5) fixed itself at the balance pan (8), located under the test chamber. There are two horizontal parallel plates connected by four screws and placed on the balance, in between these two plates the temperature regulation controller (7) is placed. The wire of the Peltier module and the thermistor inserted in the active plate (1) walk along the axis and are connected to the temperature controller. The balance is put on a mobile platform, a trolley (9) which makes it possible to slide the whole system on a rail (10) parallel to the direction of the flow. This device allows a continuous signal acquisition

recorded by a precision balance (Mettler 30, precision of ± 0.1 g), for monitoring the increase in mass as the humid air will condense on the active surface. A ring made of sponge was added around the upper part of the sealant of the Peltier module in order to collect the drops that were produced on the vertical side of the plate. Otherwise the drops would flow down by gravity and eventually fall on the heat sink or the lower surface of the test cell and then evaporate as these surfaces are warmer. As a result part of the produced mass would disappear. However, such an absorption ring has an obvious influence on the flow that develops over the plate and thereby on the condensation conditions.

Hence, on the cold side a temperature difference $\Delta T_s = T_d - T_s$ with the dew point (T_d) can be created and induce condensation [16], see Figure 3. During the experiments the controller temperature (T_c) is imposed and thus, the thermal contrast $\Delta T_c = T_d - T_c$ with the dew point (T_d), whereas ΔT_s is induced and not known precisely. Aluminium was chosen for the plate for its high thermal conductivity in order to make the active surface to be as isothermal as possible and for its corrosion properties. It is noteworthy that the size of the aluminium plate should be small enough for the active surface to be considered thermally homogeneous and large enough for the amount of condensate to be weighed accurately on an electronic balance [14].

1.3 Characterization of Condensation Surface

For the measurement procedure, the control of the flow of condensed vapour, with the objective of operating at constant flux (steady state regime), would require a constant temperature difference between the dew point and the temperature of the upper surface of the plate.

The experiments conducted for the investigation of the homogeneity of the temperature profile on the upper surface of the square flat plate (interface with air) in dry conditions (above dew point) showed that the minimum variation of temperature, over the whole surface, was 0.6°C and the maximum was 2.4°C with same size plate on the Peltier (depending on thermal differences imposed or flow) and the maximum was up to 3.5°C without plate (measured directly on the ceramic of the Peltier module) as in Figure 4b. A slightly higher temperature difference imposed in a configuration with the 3 mm plate depicts a 1.4°C surface difference only. It has been experienced here that the increased mass helps to reduce the thermal in-homogeneity on the surface of the plates. Moreover, local temperature measurements of points spread all over the surface indicated similar behaviours in time when the thermal constraints varied (T_c and/or T_d).

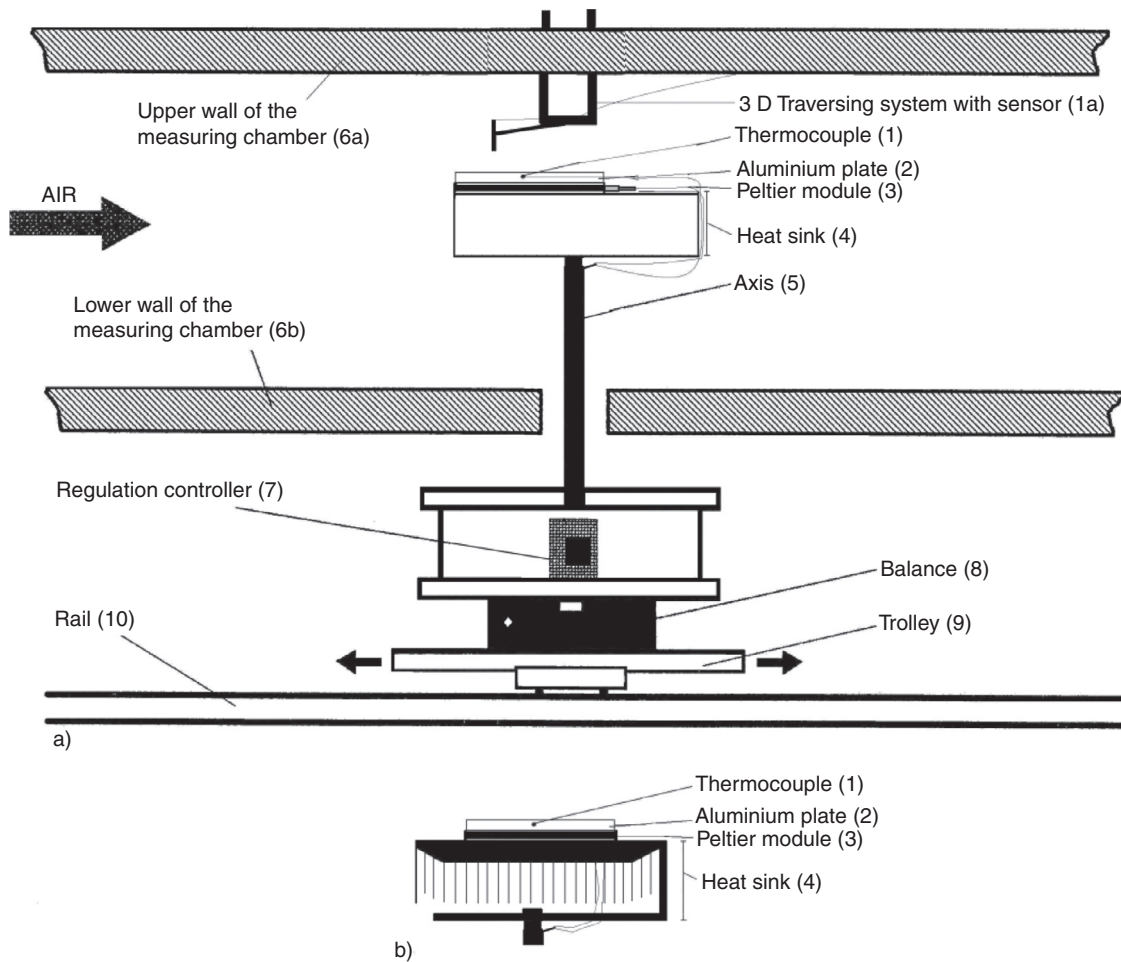


Figure 2

Sketch of the whole set-up: a) front view of the system; b) side view of the upper part which faces the airflow.

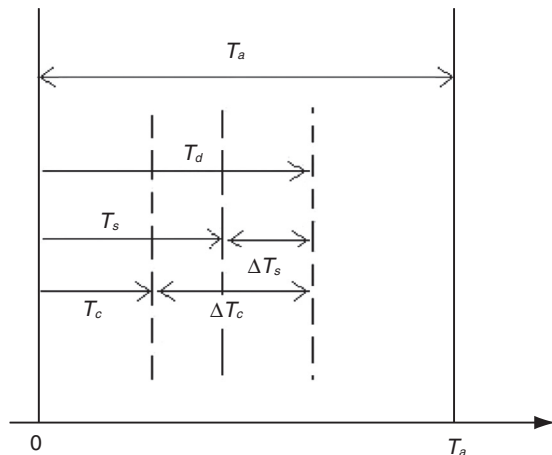


Figure 3

Different temperature levels and thermal contrasts considered herein.

The area of the plate also plays a role; an increase (from $3 \times 3 \text{ cm}^2$ to $5 \times 5 \text{ cm}^2$) helped us to produce more condensate without significantly affecting the in-homogeneity, as only minor changes were seen. It was also observed that adjusting the size of the plate to the one of the Peltier element helped in reducing the in-homogeneity of the surface of the plate.

The sample frequency of the fan for the generation of the flow inside the wind tunnel was chosen from 5 Hz to 40 Hz. The hot wire sensors available were calibrated at room temperature for velocity measurements, and the mean flow velocities chosen ranged between 1.0 ms^{-1} to 3.0 ms^{-1} with an accuracy of 1-3%. A three dimensional traversing system was used for the localization of the hot wire probe for data acquisition and the average velocity fluctuation was ensured using a computer connected to the system.

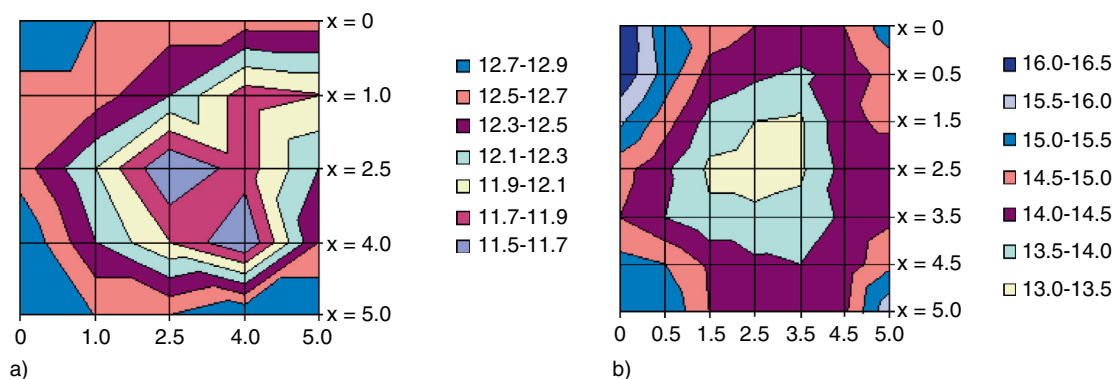


Figure 4

Temperature distribution at the solid/air interface: a) on a 3 mm plate; b) on ceramic.

1.4 Mass Condensate Measurement Method

The condensing unit including the temperature controller and all accessories were placed on the balance before condensation started. The weight of the condensing unit with all the supporting devices (such as stand, wires, heat sink, and all screws to tighten up the stand, shown in the schematic Fig. 2) was approximately 7.2 kg, and with the addition of the temperature controller the balance indicated a weight of approximately 11.8 kg before the fan was turned on. It was proven during calibration process that the air flowing intensity had no influence on the weighing process once stability was reached. The least count of the balance was 0.1 g with a maximum balance limit of 30 kg. As it is shown in Figure 2b the front face of the condensing unit was 7.5 cm wide and 6.7 cm high (or thickness). In this way, the flow of air was used to cool down the fins of the heat sink and to dissipate the heat produced by the thermoelectric elements.

The controller temperature (T_c) was chosen relatively to the dew point temperature. The value of $\Delta T_c = T_d - T_c$ was selected such that, a sufficient amount of condensate could be produced at the end of the experiment. In fact, condensation occurs when $\Delta T_s \geq 0$, but the thermal difference within the condensation interface and the temperature measured just below the top of the upper surface of the plate need to be counted for, even though it is not known. Once the process of condensation had started it was continued regularly till the end of the experiment without apparent interruption. The electronic balance showed an increase in weight, and this evolution in weight of condensate was recorded in two different ways: (i) every 30 minutes, (ii) the time was recorded every 0.1 g mass increase (upon stability). An example of mass growth acquisition *versus* time according to (i) method is presented in Figure 5;

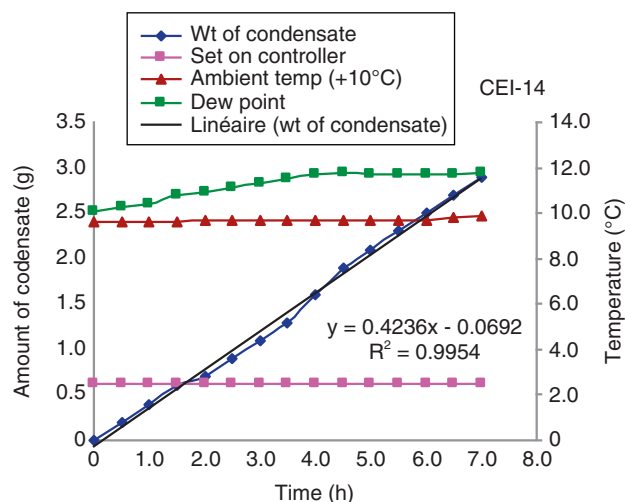


Figure 5

Plot of amount of condensate and secondary Y-axis as temperature ambient ($T_a - 10^\circ\text{C}$ plotted), dewpoint, and the temperature set on controller with respect to time.

the other key environmental parameters are presented: the ambient temperature ($T_a - 10^\circ\text{C}$ plotted), the dew point and the temperature constraint (T_c). This experiment gives a difference of linear square data fit of $0.42 \text{ g}\cdot\text{h}^{-1}$. The experimental conditions were not constant during the whole time, as one can observe from Figure 5 that the ambient temperature was quasi-constant but the dew point increased due to an increase in the relative humidity of the daily atmosphere. The increasing tendency in the dew point only lasted 4 h, and then became constant. This variation in an environmental parameter affected the rate of condensation for that particular time. Similar plots were drawn for each experiment with linear least square data fits to deduce the gradient of mass with respect to time.

2 RESULTS AND DISCUSSION

We focus in this paper on condensation experiments carried out in a wind tunnel of controlled psychrometric parameters ($\pm 0.1^\circ\text{C}$) such as relative humidity, ambient temperature and dew point. The goal was to validate the setup in a controlled environment (particularly precise weight acquisition) and finally the evaluation of the local mass transfer coefficients. Preliminary investigations in a room with no air-conditioning system, *i.e.* where the ambient environment changed according to the external weather conditions, have already been performed [15]. The goal was first to characterize each element of the design, to select the substrate (material, size, thickness and preparation), heat sink (material, size, and suitability for use in the wind tunnel and outside), and to calibrate the measurements of all the various sensors and second to validate that specific experimental concept for the evaluation of mass transfer coefficients.

2.1 Amount of Condensate Versus Time

More than 70 condensation experiments were performed on the horizontal plate at ambient temperature. Various condensation conditions (RH varied from 35% to 65%) were simulated at room temperature (around 20°C); the mean flow velocity ranged from 1 to 3 m/s. It corresponds to Reynolds numbers between 3.10^3 and 10^4 , where:

$$\text{Re} = \left(\frac{\rho_\infty UL}{\mu_\infty} \right)$$

with $L = 5$ cm and the Schmidt number was approximately 0.6, where:

$$\text{Sc} = \mu_\infty / (\rho_s D)$$

The experiments lasted from 3.5 to 8 h after condensation started. The maximum amount of condensate collected was 4.8 g on the plate and the minimum 0.8 g. The temperature and hygrometry of the wind tunnel were controlled well enough, except if there was a very large variation in the exterior ambient weather conditions (humidity or temperature), a noticeable variation in internal parameters was seen accordingly. The experimental setup of the wind tunnel was situated at INRA-Theix: $45^\circ 45' 51''$ N, $3^\circ 6' 1''$ E, and with a height of 852 m from sea level.

Figure 6 shows how the amount of collected condensate is significantly affected by a variation in different environmental parameters. The plots show the amount of condensate *versus* time for average temperature differences ΔT_c in a controlled environment. The trends

are slightly affected by the hygrometric conditions, which are not fully stable. However, both Figures 6a and 6b indicate that on increasing the temperature difference, the average rate of collection of condensate also increases accordingly. Consequently, the main trend reflects the sensitivity of the slope and, thus, of the mass flux to the temperature difference as expected. As an example, on the day of CEI-1, the dew point increased for almost 3 h and ΔT_c went up to 5.7°C , then stabilized for 1 h, and finally decreased down to 4.6°C . After more than 7 h, 2.3 g of condensate were collected on the plate, with an average ΔT_c value of 5.3°C , and an average fluctuation of $\pm 0.6^\circ\text{C}$. The other plots could be detailed the same way; Figure 6b represents the outcomes for several average ΔT_c values. All condensation rates reflect roughly linear global growths with time, whose slope increases with ΔT_c , as it generates the driving force through the partial pressure gradient.

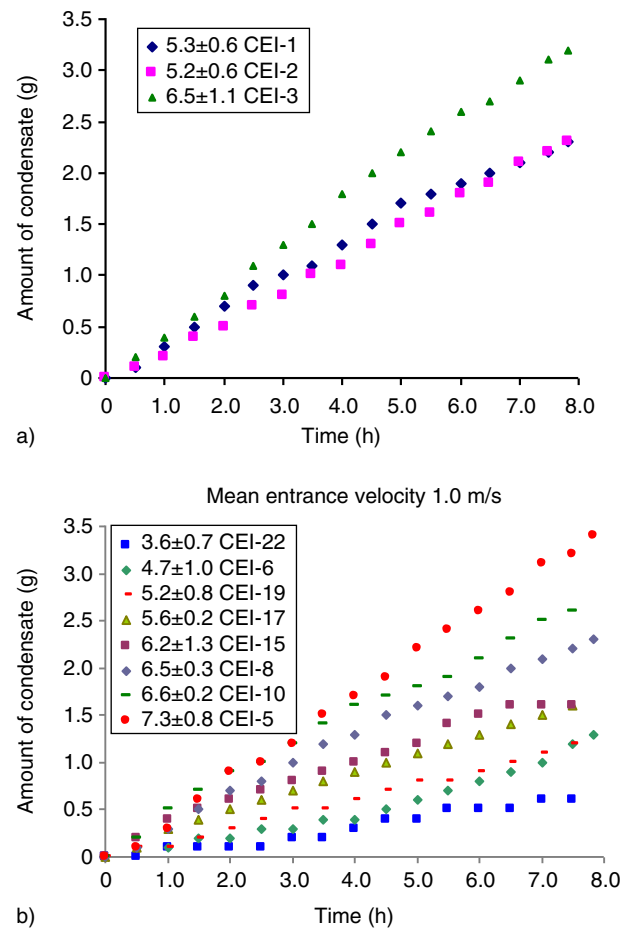


Figure 6

Amount of condensate as a function of time for different average temperature differences (ΔT_c), both are for the 1.0 m/s mean entrance velocity.

From all those plots we can deduce an average speed of condensation in various environmental conditions. These values are further used to deduce the mass flux on the plate.

2.2 Condensation Patterns

Dropwise condensation occurred every time and it was visible (very small drops in size) after a few minutes of condensation conditions. Eye observations showed that inhomogeneous distributions of drops were observed spatially and also in size. The initial growth of drops and the coalescence process were found to be as described by Beysens [17], in which bigger drops attract the smaller ones that have grown in their vicinity and thus sweep off the metal surface around which allows the condensation process to continue with the nucleation of tiny drops, etc. It results in the appearance of very different sized drops on the surface.

The surface of the aluminium metal flat plate was not well polished and only mechanical filing was done on the edges, and then just cleaned with ethyl alcohol by wipe out the substrate before starting each experiment. The hand filing of the substrate probably caused the drops to grow first on the edges all around the plate, as seen in Figure 7.

That experiment considered a mean velocity of 1 m.s^{-1} and it was a good representation of the various observations, as very scattered drop configurations were obtained. The nature of the flow had probably a major effect on those patterns, and then on the heat-mass transfer at the surface of the plate, which shows that a perfect understanding of the global phenomena would require an accurate description of the 3D flow field above the plate, but it was not our initial purpose.

It is also worth noting that the shape of the condensate is strongly influenced by the physico-chemical properties of the aluminium plate (contact angle, etc.).

2.3 Surface Temperature Estimation

The calculation of the condensation mass flux involves the partial pressure difference at the liquid/air or metal/air interface where condensation proceeds, the area of the interface and the correlated mass transfer coefficient. As usual the area is not known and the goal is to determine the $k_L.A$ coefficient. The partial pressure of the air is deduced from the ambient temperature and the relative humidity, whereas neither the pressure nor the temperatures are known. Moreover, the only accurate data available is T_c which is the temperature measured by contact with the thermistor inserted 1 mm

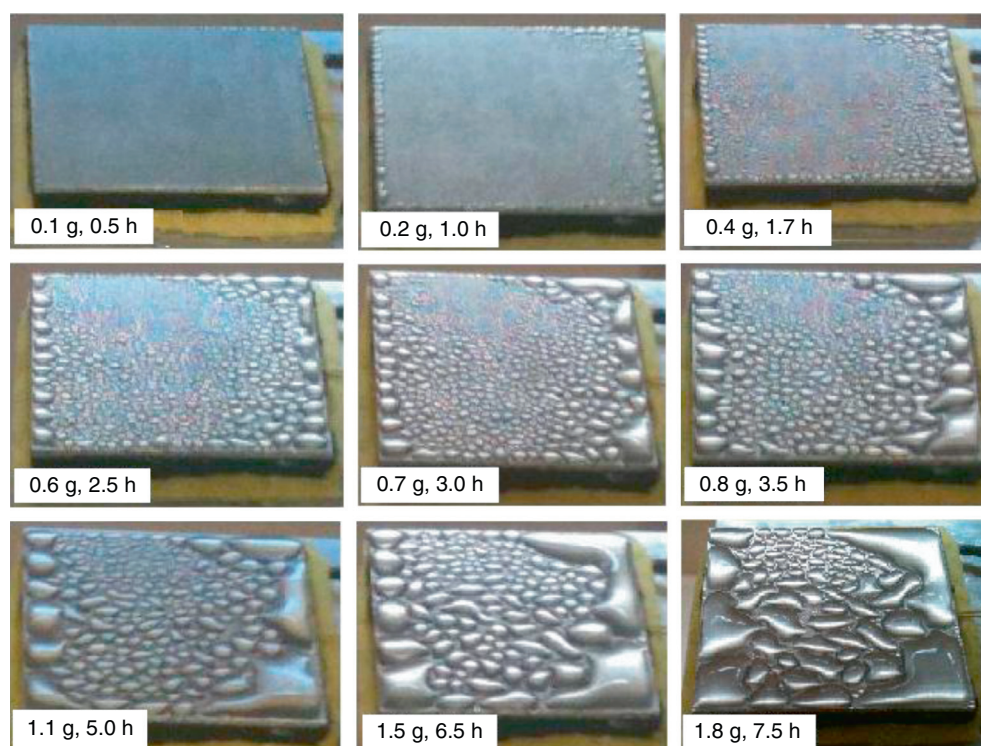


Figure 7

Photographs of the flat plate covered with condensation at different instants of an experiment.

below the metal/air surface. Modeling could have given some insights into the thermal gradient in the plate thickness and on its surface, and within the volumes (drops, masses) of condensate. But this is a 3D transient problem that involves change of phase (mass flux again), and turbulent flow modeling.

Consequently, the knowledge of the surface temperature T_s of the active condensing plate became an important task for the estimation of the mass transfer coefficient relative to condensation of humid air, in addition to the mean values of the controller temperature T_c and of the ambient temperature T_a . Moreover, the temperature set on the controller proved to be slightly smaller than just above at the interface with the air, and that there was some discrepancy in T_s over the flat plate (about 1°C) in dry air, which means that such an inhomogeneity was probably reinforced by the heterogeneous mass transfer that developed on the plate. The use of a surface sensor was not convincing because of the presence of forced convection [16]. This complexity encouraged us to try a few rules to estimate the surface temperature, keeping in mind that $T_c \leq T_s \leq T_a$. For the positive speed of condensation on the active plate, $\Delta T_s = T_d - T_s$ should be positive, we have tested:

$$T_s = T_c + T_a/2 = T_c + 0.5(T_a - T_c) \quad (1)$$

$$T_s = 3T_c + T_a/4 = T_c + 0.25(T_a - T_c) \quad (2)$$

$$T_s = 5T_c + T_a/6 = T_c + 0.16(T_a - T_c) \quad (3)$$

T_s calculated by Equation (1), led sometimes to negative temperature differences (ΔT_s), whereas a positive rate of condensation was observed in the experiments. Equation (2) induced a similar effect in a few experiments. That effect was not reached with Equation (3), the estimated T_s resulted in positive ΔT_s for every experiment with a positive speed of condensation.

Incropera and DeWitt [18] suggested, for the evaluation of all the liquid properties in the Nusselt analysis (vertical filmwise condensation), to consider the film temperature as:

$$T_f = (T_{sat} + T_s)/2 \quad (4)$$

where T_{sat} is the saturation temperature and T_s is the surface temperature. On using this rule with $T_{sat} = T_d$, $T_s = T_c$, we have calculated the surface temperature as:

$$T_s = (T_d + T_c)/2 \quad (5)$$

and found that this value is approximately ($\pm 1.0^\circ\text{C}$) equal to the one calculated with Equation (3).

In heat transfer problems and for the evaluation of the Nusselt number in vertical configurations, Minkowycz

and Sparrow [19] proposed the use of a reference temperature defined by:

$$T_{ref} = T_c + 0.31(T_a - T_c) \quad (6)$$

The authors also reported that for the estimation of heat transfer coefficient the Nusselt model gave a good agreement with their results taking into account variable physical properties evaluated with that reference temperature.

We have also considered two “limit” cases to calculate T_s :

$$T_s = T_c + 1.0 \quad (7)$$

$$T_s = T_d \quad (8)$$

Indeed, Equation (7) gives an approximate of the minimum possible surface temperature according to our surface temperature investigation in dry air conditions, and Equation (8) gives a maximum possible temperature for condensation to start, as the condensation can only occur when $T_s < T_d$.

2.4 Mass Flux Evaluation for a Mean Flow Velocity of 1 m.s⁻¹

Finally we used Equation (3) to estimate the surface temperature T_s , and thus, we could deduce the mass flux on the plate by considering the area of the plate (5 cm × 5 cm) as the mass transfer exchange surface.

The dependence of the mass flux as a function of the average temperature difference ΔT_s is depicted in Figure 8a, and as a function of the mean difference in partial pressure (between the saturated vapour partial pressure of the mean flow and the partial pressure at T_s) in Figure 8b. Each experimental point corresponds to a 6-8 h experiment. The experimental value results from the algebraic average over the whole experiment duration of the data points evaluated at each time of measurement; the “slope” corresponds to the gradient of the curves plotted for the increase in weight with time for each experiment [15] (see Sect. 2.3 and Fig. 5).

The improperly called “theory” data correspond to the arithmetic mean of points calculated using the environmental data recorded at the time of the experiment and by assuming a heat/mass analogy for the mass flux evaluation of a simple 1D stationary model. The heat flux is the one that would be calculated for a flat horizontal plate covered by a film of condensate when a laminar boundary layer flow develops on top [16].

The theoretical data show the best fits, particularly in Figure 8b (Δp). The data are more scattered in Figure 8a, particularly for the calculated ones, which indicates that the difference in partial pressure is a better indicator

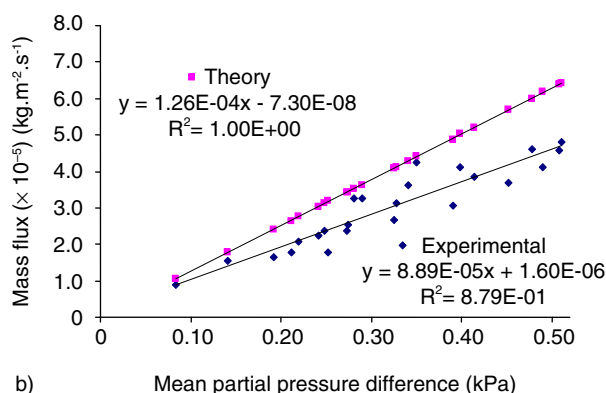
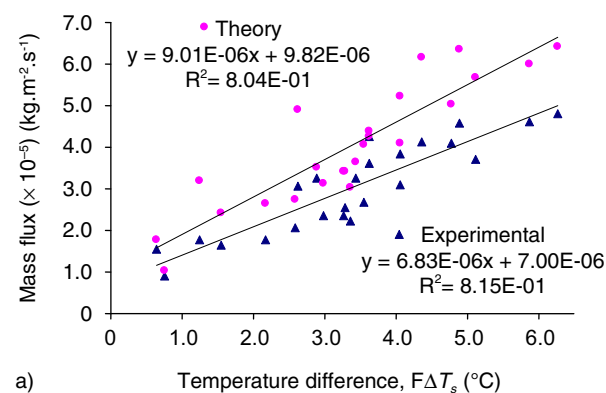


Figure 8

Mass flux for a mean entrance velocity of 1.0 m/s as a function of: a) the temperature difference (ΔT_s), b) the mean partial pressure difference.

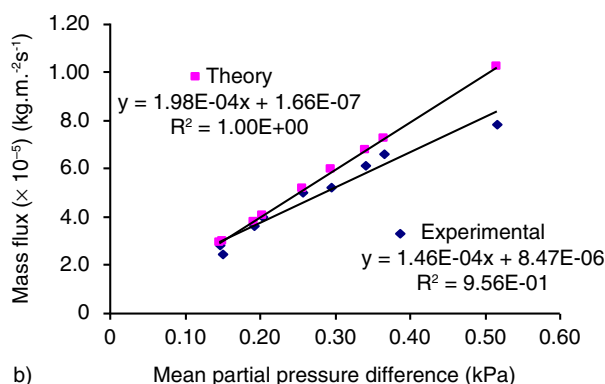
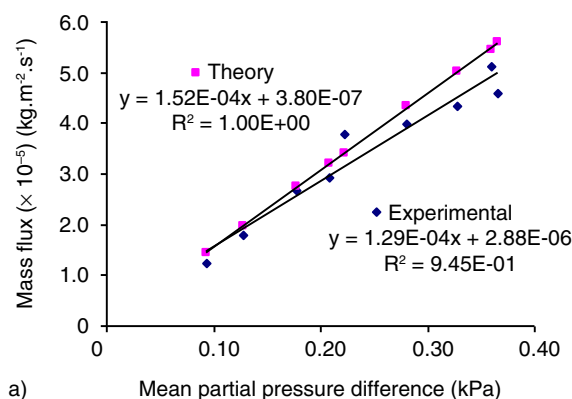


Figure 9

Mass flux as function of mean partial pressure difference (kPa) for a mean entrance velocity of a) 1.5 m/s and b) 2.5 m/s.

than the difference in temperature for the estimation of the mass flux. Indeed the driving force for condensation mass transfer (controlled by the diffusion of water vapour towards the condensation interface) is better modelled by partial pressure differences than temperature differences solely (no interaction with the relative humidity which is a key factor, as minor deviation in RH level (5% is enough) during an experiment influence significantly the condensation rate; such an effect cannot be counted for when only ΔT_s are considered). As a matter of fact, a long variation in RH would act as a spurious mode, as the global problem is multi-parametric and the bi-dimensional plots given herein can only deal with 1 to 3 parameters only.

For the experimental data, variations in the experimental conditions can justify most of the scattering in data. The global experimental set up did not allow us to be more precise and to conduct experiments at a specific ambient temperature coupled with a specific relative humidity over 7 h as, even sealed and insulated, the air in

the closed loop was slightly affected by outside environmental conditions after a few hours.

2.5 Influence of the Mean Entrance Velocity

An increase in the air flow intensity to 1.5 and further to 2.5 m.s⁻¹ is described in Figure 9. The mass flux variations show trends more or less similar between the experimental data and the modeled ones. In both cases, but it is noticeable with fewer data, the scattering is much reduced for partial pressure difference and temperature difference as well.

The theoretical data in Figure 9b reflect 100% linearity in the mass flux *versus* the partial pressure difference plot shows, and 95-96% for the experimental ones. The gradient of mass flux with partial pressure difference keeps increasing and amounts to 1.29×10^{-4} in the experiments and 1.52×10^{-4} for the theory (18% more) at 1.5 m.s⁻¹. That increase gets higher at 2.5 m.s⁻¹, as it reaches 1.46×10^{-4} and 1.98×10^{-4} with the model

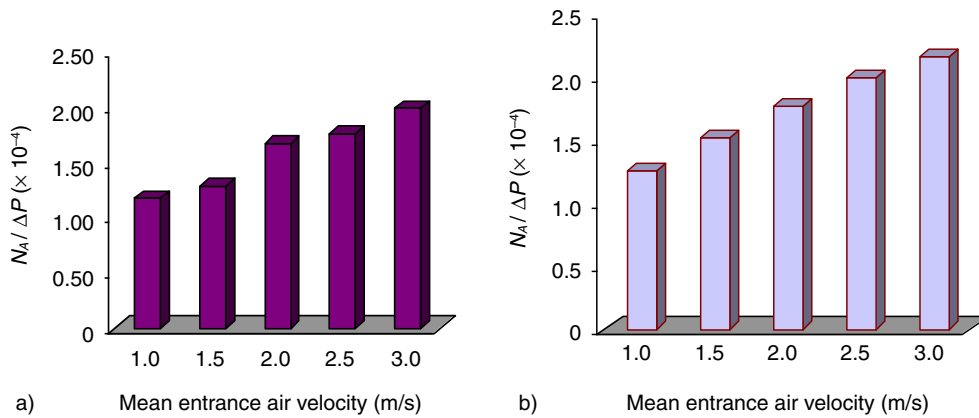


Figure 10

Plots of $N_A/\Delta p$ as a function of the mean entrance velocity for the a) the experimental data, and b) the theoretical data.

(almost 36% more). When increasing the flow intensity further similar results were found; the gradient of mass flux with temperature difference is always lower than with partial pressure difference; also the theoretical values are always higher than the experimental ones.

In addition, we found that, for the studied $1\text{--}3\text{ m.s}^{-1}$ velocity range, the regression coefficients of the mass flux with partial pressure difference reached nearly 100% fit for the theory, and slightly less for the experiments. In opposition, the regression coefficients for the temperature difference plots were most of the time higher for the experimental data than for the theoretical ones. For 1.0 m/s (Fig. 8) many more data were available, but these data covered more variations in physical environmental conditions: ΔT_c was in the range $3.4\text{--}9.8^\circ\text{C}$, while the relative humidity was in $43\text{--}63\%$ for a total of 24 data points. For 1.5 m/s , ΔT_c was in $3.3\text{--}8.2^\circ\text{C}$ and RH in $38\text{--}48\%$, with a total of 9 data points only.

On increasing the mean entrance velocity inside the wind tunnel, the mass flux has a tendency to increase but not according to a linear variation. The histogram shown in Figure 10a corresponds to the variation of the mass flux (N_A) with respect to the mean partial pressure difference as a function of the mean entrance velocity for the experimental data, and in Figure 10b for the calculated data. Scattered experimental data have been removed to reduce the discrepancy.

On those plots one can read the mass transfer coefficients we investigated for condensation over a horizontal plate. The imposed temperature difference, ΔT_c , in the experiments were chosen in the range 1.2°C to 4.1°C , which was quite low in comparison to the regulated environment of the wind tunnel. Figure 10a (experimental

data) shows a mass flux coefficient for 2.0 m/s with a higher value in comparison to the other entrance velocities. It was caused by the higher temperature differences chosen during these condensation experiments and durations of a few experiments, the physical environmental parameters have recorded large variations for this specific velocity. Figure 10 establish clearly the raise in the mass transfer coefficients on increasing the velocity inside the wind tunnel, that result was expected as on raising the flow intensity the condensation surface faces stronger convective flows and thus the diffusion layer that develops above the condensation interface should be getting thinner.

Nevertheless, during these measurements the range of the average physical parameters was not the same.

CONCLUSION

The modeling of a closed ecological life support system for space flights or space bases requires apprehending the air flow conditions (quality, hydrodynamics, heat transfer, humidity transfer, CO_2 concentration, O_2 concentration, etc.) in order to improve the living conditions and maintenance and particularly gas/liquid transfer exchanges at interfaces. Such a complex modeling is based on local mass transfer coefficients. We have developed an experimental setup and protocol to measure such coefficients for specific geometries in a well controlled environment (climatic wind tunnel) on Earth. The use of thermoelectricity to produce a homogeneous surface temperature coupled with a precise weighing for the condensation of humid air on a small size substrate

proved to be efficient for the evaluation of local mass transfer coefficients. This study focused on the characterization of condensation on a flat horizontal plate of small size in a low Re number turbulent flow, which corresponds to configurations that can be encountered in many applications, on earth and in space where condensation remains a major concern (greenhouse, manned capsule). The variation of the mean flow velocity inside the wind tunnel showed an expected significant effect on the mass transfer coefficients.

ACKNOWLEDGMENTS

The authors are thankful to the Centre National d'Études Spatiales (CNES, France) and the European Space Agency (ESA) for providing financial support.

REFERENCES

- De Micco V., Buonomo R., Paradiso R., De Pascale S., Aronne G. (2012) Soybean cultivar selection for Bioregenerative Life Support Systems (BLSS) – Theoretical selection, *Adv. Space Res.* **49**, 10, 1415-1421, DOI:[10.1016/j.asr.2012.02.022](https://doi.org/10.1016/j.asr.2012.02.022).
- Zimmerman R. (2003) Growing pains, *Air Space Magazine*, Sept., pp. 31-35.
- Perchonok M., Bourland C. (2002) NASA food systems: past, present, and future, *Nutrition* **18**, 913-920.
- Salisbury F.B., Gitelson J.I., Lisovsky G.M. (1997) Bios-3: Siberian experiments in bioregenerative life support, *Bioscience* **47**, 575-585.
- Wolverton B.C. (1980) Higher Plants for Recycling Human Waste into Food, Potable Water and Revitalized Air in a Closed Life Support System, *Earth Resources Laboratory, National Aeronautics and Space Administration*, NASA-TM-87550.
- Wignarajah K., Pisharody S., Fisher J.W. (2000) Can incineration technology convert CELSS wastes to resources for crop production? A working hypothesis and some preliminary findings, *Adv. Space Res.* **26**, 327-333.
- Zolotukhin I.G., Tikhomirov A.A., Kudenko Y.A., Gribovskaya I.V. (2005) Biological and physicochemical methods for utilization of plant wastes and human exometabolites for increasing internal cycling and closure of life support systems, *Adv. Space Res.* **35**, 1559-1562.
- Gros J.B., Poughon L., Lasseur C., Tikhomirov A.A. (2003) Recycling efficiencies of C,H,O,N,S, and P elements in a biological life support system based on micro-organisms and higher plants, *Adv. Space Res.* **31**, 195-199.
- Mergetay M., Verstraete W., Dubertret G., Lefort-Tran M., Chipaux C., Binot R. (1988) MELISSA - a microorganisms based model for CELSS development, *3rd symposium on space thermal control & life support system*, Noordwijk, The Netherlands, 3-6 Oct.
- Yabuki K., Miyagawa H. (1970) Studies on the effect of wind speed on photosynthesis, *Jpn. J. Agric. Meteorol.* **26**, 137-142. (in Japanese with English summary).
- Monteith J.L., Unsworth M.H. (1990) *Principles of Environmental Physics*, Edward and Arnold Publishing Co, London, p. 291.
- Kitaya Y., Shibuya T., Yoshida, Kiyota M. (2004) Effects of air velocity on photosynthesis of plant canopies under elevated CO₂ levels in a plant culture system, *Adv. Space Res.* **34**, 7, 1466-1469.
- Tiwari A., Fontaine J.P. (2009) Towards the prediction of heat & mass transfer in an air-conditioned environment for a life support system in space, *Water Air Soil Poll. Focus* **9**, 5-6, 539-547.
- Tiwari A., Lafon P., Kondjoyan A., Fontaine J.P. (2010) Experimental modelling for the prediction of heat and mass transfer in an air-conditioned space environment for life support systems, *40th ICES-2010*, Barcelona, Spain, AIAA2010-6171
- Tiwari A., Lafon A., Kondjoyan A., Fontaine J.P. (2011) An air-conditioned wind tunnel environment for the study of mass and heat flux due to condensation of humid air, Chapter 4, *Wind Tunnels: Aerodynamics, Models and Experiments*, Pereira J.D. (ed.), Nova Science Publishers, Inc., New York, USA, ISBN: 978-1-61209-1.
- Tiwari A. (2011) Characterisation of mass transfer by condensation of humid air on a horizontal plate, *PhD Thesis*, Blaise Pascal University, Clermont-Ferrand, France.
- Beysens D. (2006) Dew nucleation and growth, *C. R. Physique* **7**, 1082-1100.
- Incropera F.P., DeWitt D.P. (1990) *Fundamentals of Heat and Mass Transfer*, 3rd edn., John Wiley & Sons, Inc., New York.
- Minkowycz W.J., Sparrow E.M. (1996) Condensation heat transfer in the presence of noncondensables, interfacial resistance, variable properties and diffusion, *Int. J. Heat Mass Trans.* **9**, 1125-1144.

Manuscript accepted in April 2013

Published online in December 2013